

In-silico* approach to identify novel potent inhibitors against GraR of *S. aureus

Poonam Dhankhar¹, Vikram Dalal¹, Dasantila Golemi-Kotra², Pravindra Kumar¹

¹Department of Biotechnology, IIT Roorkee, Uttarakhand-247667, India, ²Department of Biology, York University, 4700 Keele Street, Toronto, Canada

TABLE OF CONTENTS

1. Abstract
2. Introduction
3. Material and method
 - 3.1. Homology modeling
 - 3.2. Virtual screening
 - 3.3. IC₅₀ and molecular properties calculations
 - 3.4. Molecular docking
 - 3.5. Molecular dynamics simulation
 - 3.6. MMPBSA binding free energy calculation
4. Results
 - 4.1. Homology modeling
 - 4.2. Virtual screening
 - 4.3. IC₅₀ and molecular properties calculations
 - 4.4. Molecular docking
 - 4.5. Molecular dynamics simulation
 - 4.5.1. Root mean square deviation (RMSD)
 - 4.5.2. Root Mean Square Fluctuation (RMSF)
 - 4.5.3. Radius of gyration (Rg)
 - 4.5.4. Solvent Accessible Surface Area (SASA)
 - 4.5.5. Hydrogen bond analysis
 - 4.6. MMPBSA binding free energy calculation
5. Discussion
6. Conclusion
7. Acknowledgments
8. References

1. ABSTRACT

With rising antibiotic resistance at alarming rates in *S. aureus*, a major human pathogen, it is important to identify targets for new antimicrobial therapies. A number of two-component systems (TCS) have been implicated in *S. aureus* resistance to several antibiotics. The glycopeptide-resistance associated TCS, GraSR, is involved in cationic antimicrobial peptides (CAMPs) resistance through the regulation of *mprF*, *dltABCD*, and *vraFG* operons.

GraS is a sensor histidine kinase, while GraR is a response regulator transcription factor, which is potential drug target. In lieu of the significance of GraSR in antibiotic resistance and the lack of structural studies on GraR, we undertook to determine the GraR structure through homology modelling. A series of small molecules were virtually screened and the top-scored molecules were analyzed for different pharmacophore properties and

assessed for their binding potency to GraR (IC₅₀). Further, a molecular dynamics simulation study of GraR-ligand complexes revealed that the predicted molecules exhibited good binding affinities at the dimerization interface of GraR. Thus, these molecules could be suitable inhibitors for the GraR-mediated signalling processes, which may be further utilized to develop novel antimicrobial agents against *S. aureus*.

2. INTRODUCTION

Staphylococcus aureus is a Gram-positive coccus shaped bacterium, which is frequently found in the respiratory tract and on the skin of humans. As an opportunistic and commensal pathogen, it causes a number of diseases ranging from minor skin infections to life-threatening diseases such as pneumonia, endocarditis, meningitis, and toxic shock syndrome (1, 2). Due to the indiscriminate use of antibiotics, *S. aureus* have adapted to their use and have evolved resistance to most of the clinically used antibiotics, and are becoming a serious issue in hospital and community settings (1).

To the *S. aureus* infection, the host innate immune system uses the first line of defense to secrete cationic antimicrobial peptides (CAMP). CAMPs are amphipathic in nature, produced as a part of the host defense mechanism by the host epithelial, immune and skin cells (1, 3). Gram-positive bacteria counteract CAMPs through several resistance mechanisms, including proteolytic degradation, sequestration, cell surface modifications, and efflux. A number of these resistance mechanisms are controlled by two-component signal transduction systems (TCSs) (4). TCSs are abundantly present in bacteria and rare in archaea and eukaryotes, while markedly absent in metazoans (5).

Different bacterial species harbor various TCSs that are specialized in responding to a particular environment signal, such as pH, nutrient levels, osmotic pressure, redox state, quorum-sensing proteins, and antibiotics (6). Therefore, TCSs are perceived as attractive and potential

targets for the development of novel antibacterial drugs. A specific inhibitor of TCS may be more effective than conventional antibiotics due to its unique mechanism of action; a specific TCS inhibitor is likely to have a narrow spectrum of action, hence the incidence of resistance may affect one pathogen but not the others (7).

In general, TCSs consists of a membrane-bound histidine kinase (HK) that acts as a sensor kinase and a cytoplasmic response regulator (RR) that often functions as a transcriptional regulator (6). The histidine kinase of a TCS responds to the external signal via its autophosphorylation and relays the information to RR through a phosphotransfer process that commences the cellular responses (5). A RR consists of a conserved N-terminal receiver domain (RD), which harbors the site for phosphorylation, a conserved aspartate residue, by its cognate histidine kinase, and a variable C-terminal effector domain (ED) which has a DNA binding motif (8). RRs exist in equilibrium between the active and inactive conformation, with the receiver domain serving as a molecular switch (9). The phosphorylation of the conserved aspartate residue causes structural and conformational changes that result in dimerization of the receiver domain and exposure of the DNA-binding motif in the ED (5, 8).

S. aureus resistance against CAMPs involves the increase of the positive charge on the bacterial cell surface. TCS GraSR mediates the modification of the bacterial cell surface charge. This TCS senses the presence of these peptides and regulates among the others, the expression of the operons *mprF* and *dltABCD*. Activation of these two operons leads respectively to the lysinylation of phosphatidyl-glycerol embedded into the cytoplasmic membrane and the D-alanylation of wall teichoic acid (WTA), which ultimately results in an overall positively charged cell surface. GraSR consists of GraS, a membrane-bound sensor kinase and GraR, a cytoplasmic response regulator that acts as a transcriptional regulator (6). In response to an extracellular signal(s), it is thought that GraS undergoes autophosphorylation at a conserved His residue in its cytoplasmic domain and thus it becomes active. Subsequently, to transduce the

signal, the phosphoryl group of GraS is transferred onto a specific conserved aspartate residue of the receiver domain of GraR, Asp51. This phosphorylation step dimerizes GraR and modulates its transcriptional regulatory activity (6). Activation of GraR provides the resistance to *S. aureus* for CAMP through repulsion and expulsion mechanism (10). GraSR is also linked to the virulence and cell-wall metabolism (10). Sequence alignment analysis suggests that GraR belongs to the OmpR/PhoB family of RRs, which utilizes the conserved alpha4-beta5-alpha5 motif as the dimerization interface during their phosphorylation-induced activation (11, 12). Inhibition of the phosphorylation-induced dimerization in response regulators by small molecules was proposed as an effective way of inhibiting bacterial signal transduction (11). The 3-dimensional structure of GraR is not known; hence, it is unclear how the phosphorylation induced activation of GraR occurs. In this study, we used homology modeling to predict the 3-dimensional structure of GraR for the screening of novel compounds via virtual screening. Pharmacophore properties were assessed for the screened molecules. Molecular docking program AutoDock Tools and AutoDock Vina result infer that five novel compounds (ZINC000049170029, ZINC000095509204, ZINC000067688459, ZINC000049169934, and ZINC000095352231) interact with GraR with high binding affinities. These molecules are stabilized by hydrogen bonding, polar interaction, and hydrophobic interaction. In order to evaluate the interactions of these molecules with GraR, each respective complex was subjected to molecular dynamics (MD) simulation and molecular mechanic/Poisson-Boltzmann surface area (MMPBSA) binding free energy calculations. Our study suggests that these five novel molecules have the potential to interact *in vivo* with GraR.

3. MATERIAL AND METHOD

3.1. Homology modeling

Homology modeling was performed to construct the 3D structure of the GraR protein because its crystal structure is not available.

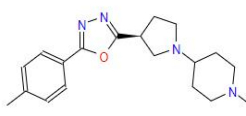
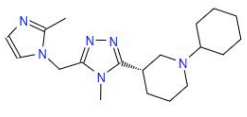
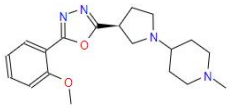
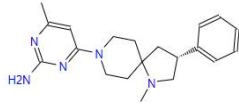
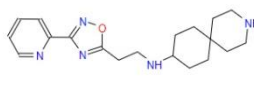
Therefore, the GraR protein sequence from *S. aureus* was retrieved from UniProt database (UniProtKB - Q932F1) and the NCBI BLAST tool was used to determine the homologous structures (13, 14). The multiple sequence alignment of GraR from *S. aureus* with other homologous proteins, the structures of which are known, were generated using Clustal Omega and analyzed using ESPript3 (15, 16). Domains and motifs of GraR were assessed using various online tools and databases like InterPro, Prosite, and NCBI-Conserved domain database (17-19). The 3D homology model of GraR was predicted using the SWISS-Model server (<https://swissmodel.expasy.org/>) (20). Its calculation depends on the importance of threading template alignments and also the convergence parameters of the structure assembly simulations. The refinement of the disordered loops was performed using MODLOOP (21). The SWISS-PDB viewer was utilized for energy minimization of the modeled structure (22). The minimized model was validated by assessing the stereochemical quality using the various tools of SAVES server (<http://nihserver.mbi.ucla.edu/SAVES/>) such as PROCHECK, VERIFY3D, ERRAT and ProSA (23-26). PyMOL and chimera were used to visualize and analyze the validated model (27, 28). Furthermore, 3D-predicted model was validated by molecular dynamics using GROMACS 5.14 suite along with GROMOS54a7 force field on an Ubuntu-based workstation (29, 30).

3.2. Virtual screening

Drug-like molecules were retrieved from ZINC DATABASE (<https://zinc15.docking.org/>) (31). Ligands were energy minimized by Universal Force Field (UFF) and converted to pdbqt format using Open Babel in PyRx0.8 for virtual screening (32, 33). Virtual screening was performed using PyRx0.8 along with VINA and the predicted binding affinity was calculated in kcal/mol (34). The grid for molecular docking was centered around Met90, Gly93, Ala94, Asp95, and Arg117 of interface residues of the protein. The grid center points were set at X=-46.4, Y=6.98, Z=26.8, and dimensions were as X=27.7, Y=28.9, and Z=28.7 with exhaustiveness 8. Further, poses with the highest binding affinity and

Identification of potent inhibitors against GraR

Table 1. Chemical characterization of the hit ZINC compounds

S No:	ZINC ID	Chemical name	Chemical formula	Chemical structure
1	ZINC000049169934	1-Methyl-4-((3S)-3-(5-(4-methylphenyl)-1,3,4-oxadiazol-2-yl)-1-pyrrolidinyl) piperidine	C ₁₉ H ₂₆ N ₄ O	
2	ZINC000095352231	1-Cyclohexyl-3-(4-methyl-5-((2-methyl-1H-imidazol-1-yl)methyl)-4H-1,2,4-triazol-3-yl)piperidine	C ₁₉ H ₃₀ N ₆	
3	ZINC000049170029	4-((3S)-3-(5-(2-Methoxyphenyl)-1,3,4-oxadiazol-2-yl)-1-pyrrolidinyl)-1-methylpiperidine	C ₁₉ H ₂₆ N ₄ O ₂	
4	ZINC000095509204	4-Methyl-6-(1-methyl-3-phenyl-1,8-diazaspiro(4.5)dec-8-yl)-2-pyrimidinamine	C ₂₀ H ₂₇ N ₅	
5	ZINC000067688459	N-(2-(3-(2-Pyridinyl)-1,2,4-oxadiazol-5-yl)ethyl)-3-azaspiro(5.5)undecan-9-amine	C ₁₉ H ₂₇ N ₅ O	

the corresponding interactions were saved and analyzed in PyMOL (27).

3.3. IC₅₀ and molecular properties calculations

The pkCSM web-server was used to determine the physicochemical and pharmacokinetic parameters such as molecular weight, total polar surface area, number of hydrogen bond donors and acceptors. The *in-silico* absorption, distribution, metabolism, excretion, and toxicity (ADMET) properties have been computed using pkCSM server (35). The ADMET profile of molecules was predicted by several factors such as water solubility, skin permeability, Caco-2 permeability, Human Intestinal absorption, P-glycoprotein substrate, the volume of distribution (VDss), cytochrome P450 323 2D6 inhibition, renal OCT2 substrate, total clearance, AMES toxicity, skin sensitization. XIAPin online web server tool (<http://crdd.osdd.net/oscadd/xiapiin/>) was used to

calculate the IC₅₀ values of the most potent molecules.

3.4. Molecular Docking

The AutoDock 4.2.6. was utilized for docking of the screened molecules against GraR (36). Hydrogen atoms and Kollman charges were added on a protein using MGLTools. The hydrogen atoms and Gasteiger charges for ZINC000049170029 (1.99), ZINC000095509204 (2.00), ZINC000067688459 (2.00), ZINC000049169934 (2.00) and ZINC000095352231 (1.00) were added and saved in the pdbqt format. The chemical name and structures of the compounds are shown in Table 1. The grid map with a spacing of 0.375 Å was generated using AutoGrid4. The molecular docking grid was created around Met90, Gly93, Ala94, Asp95, and Arg117 of interface residues. The grid box dimensions and center point coordinates were set as 34 Å X 34 Å X 36 Å and -35.66, 9.138, -26.09, respectively. A Lamarckian genetic algorithm was utilized for molecular docking

and the number of conformations were increased from 10 to 50. The highest binding and corresponding interactions pose were visualized and inspected in PyMOL (27). Moreover, HADDOCK web server is also utilized for the docking of ZINC000049170029, ZINC000095509204, ZINC000067688459, ZINC000049169934 and ZINC000095352231 with GraR (37-39). The protein and ligand interactions Figures were prepared using PyMOL, Chimera, and Maestro (Schrödinger Release 2017-4: Maestro, Schrödinger, LLC, New York, NY, 2017) (27, 28).

3.5. Molecular dynamics Simulation

The atomistic dynamics and the binding stability of GraR–ligand complexes were studied using molecular dynamics simulation. The molecular simulation studies were done using the GROMOS96 54a7 force field along with SPC (simple point charges) water model in GROMACS 5.1.4. suite (29, 30). Topology of the inhibitors (ZINC000049170029, ZINC000095509204, ZINC000067688459, ZINC000049169934 and ZINC000095352231) were generated using PRODRG webserver (40). The systems were solvated in a triclinic box with a minimum of 2 nm marginal radii from the closest atom of protein and neutralize by adding the counter-ions (Na^+). The dimensions and volume of the box were 9.91 X 7.93 X 9.1 nm and 718.04 nm³, respectively. The steepest descent algorithm was used for energy minimization to reduce the steric clashes. The energy minimization was performed using 50,000 iteration steps and the energy cut off was kept up to 10.0 kJmol⁻¹. Two equilibration steps were performed: a constant number of particles, volume, and temperature (NVT) and a constant number of particle, pressure, and temperature (NPT) at 300 K. Berendsen temperature coupling method was used to regulate the temperature of the box. The first phase of the equilibration was done for 50,000 steps at 300 K; each step of 2 fs. Further, the next phase of equilibration was performed for 1 ns and coordinates were generated at every 1 ps. Particle Mesh Ewald (PME) with 1.6 Å Fourier grid spacing was used for calculation of Long-range electrostatics (41). The covalent bond constraints were done using the LINCS algorithm and coulomb interactions were calculated within a cut off the

radius of 12 Å. The molecular dynamics simulation was run for 100 ns with a time step of 2 fs each and the trajectories were generated at every 10 ps. The RMSD, RMSF, Rg, SASA, number of hydrogen bonds were generated using g_rms, g_rmsf, g_gyrate, g_sasa, and g_hbond, respectively within in GROMACS (29).

3.6. MMPBSA binding free energy calculation

The binding free energy of GraR–ligand complexes was determined using the g_mmpbsa tool (42). This software utilizes the Molecular Mechanics/Position-Boltzmann Surface Area (MMPBSA) method to calculate the binding free energy of interactions between protein–ligand complex. Here in this study, the trajectories for every 10 ps for the last 20 ns i.e. between 80 to 100 ns were collected to predict the binding energy.

4. RESULTS

4.1. Homology modeling

The GraR sequence consisting of 224 amino acids was retrieved from the UniProt in the FASTA format (UniProtKB - Q932F1). NCBI Blast tool showed that GraR exhibits maximum sequence identity of 37 percent with NsrR (nisin resistance regulator protein) of *Streptococcus agalactiae*. The secondary structure of the GraR protein was predicted using PDBsum and shown in Figure 1. The functional domain of GraR, analyzed using Prosite, showed that GraR contained two conserved domains referred to as the N-terminal (receiver) and the C-terminal (effector) DNA-binding domain. Multiple sequence alignment of GraR along with the sequences of other homologous RRs, with known structures, was performed and generated using Clustal Omega and ESPript3, respectively, as shown in Figure 2 (15, 16).

The robust 3D model of GraR was generated from Swiss-Model web-server and represented as a cartoon in Figure 3. The constructed 3D structure was subjected to energy

Identification of potent inhibitors against GraR

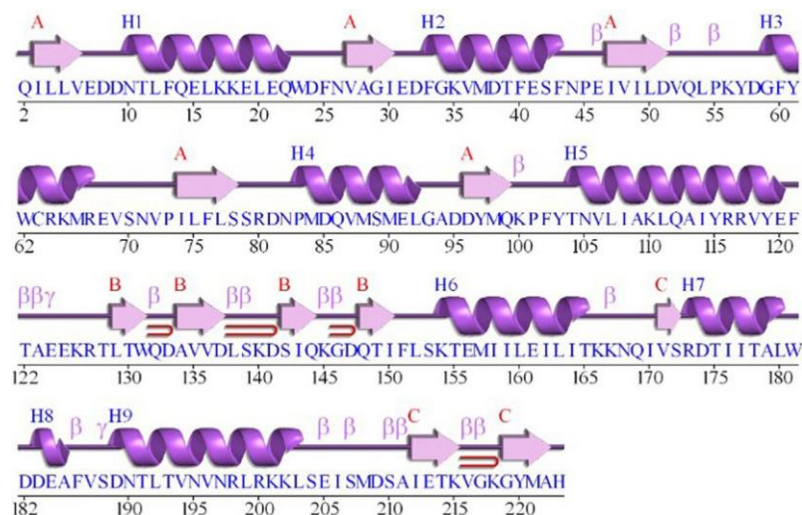


Figure 1. The secondary structure presentation of the GraR protein generated using PDBSum.

minimization using SWISS-PDB viewer, and the disordered regions were refined by ModLoop. SAVES server tools were used to check the quality and accuracy of the refined model. The Ramachandran plot of GraR generated by PROCHECK showed that 87.5 percent of the amino acid residues are in the most favoured region, 12 percent in the allowed region, and 0.5 percent in the disallowed region, as shown in Figure 4A, and Table 2. The modeled structure was analyzed using SAVES server. The quality factor of the model by ERRAT plot was 95.3 percent as shown in Figure 4B. VERIFY3D showed that the quality factor of 84.68 percent of amino acid residues has an average 3D-1D score greater than or equal to 0.2 as shown in Figure 4C. Further ProSA server gave a Z-score for the modeled and the template structure of -6.84 and -7.27, respectively. These Z-score values show that the predicted GraR structure is in good agreement with the structure of the experimentally determined homologous protein, as shown in Figure 5. The structural superposition of GraR modeled structure with the homologous structures has a Root Mean Square Deviation (RMSD) value of 0.11 Å for 181 C-alpha atoms. The model was subjected to the molecular dynamics using GROMACS. The RMSD plot shows that the model achieved convergence at 0.47 nm up to 34 ns and was stable throughout the simulation. The validated GraR model

exhibited 224 amino acids along with 9 alpha helices (alpha1-alpha9) and 12 beta sheets (beta1-beta12) as shown in Figure 3. It consisted of two domains named as the N-terminal and the C-terminal DNA binding domain. The N-terminal domain (residues 1-121) is comprised of the central parallel beta sheets (beta 1-5) surrounded by alpha-helices alpha1 and alpha5 on one face and alpha2 to alpha4 on the other side. This domain also contained the highly conserved alpha4-beta5-alpha5 motif.

Very interestingly, the alpha4-beta5-alpha5 motif was exposed to milieu. Normally, this motif is involved in intra-domain interactions in the other OmpR/PhoB proteins, such as PrrA and DrrD; interactions that hold the RR in an inactive state (43, 44). The C-terminal domain (residues 129-224) harbored the helix-turn-helix fold, which is a conserved feature among RRs and it is involved in DNA binding. This helix-turn-helix motif in GraR started with four-stranded antiparallel beta-sheets and was followed by a three-helix bundle and two stranded anti-parallel beta-sheets. Further, a loop of 7 residues (residues 122-128) connected both N- and C-terminal domains. Of note, the alpha 7-9 helices were predicted to be fully exposed to milieu by the GraR model, suggesting that unphosphorylated GraR should be able to bind to DNA. Indeed, Muzamal *et al.*

Identification of potent inhibitors against GraR

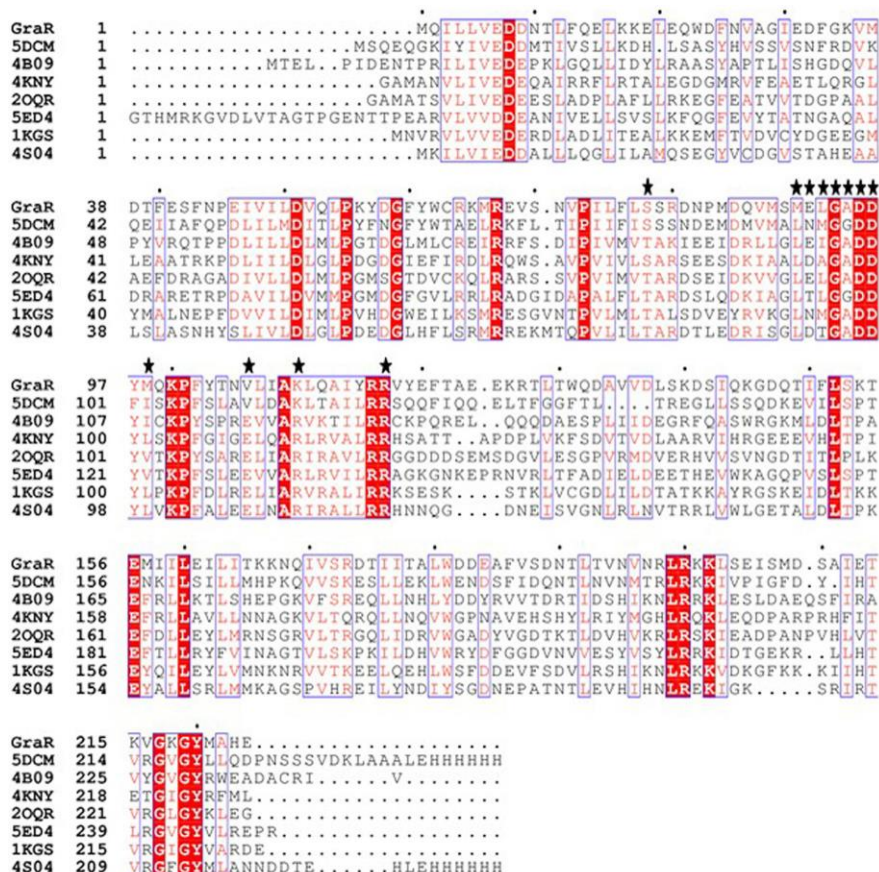


Figure 2. Multiple sequence alignment (MSA) of GraR from *S. aureus* with response regulators from different organisms. MSA was done using Clustal Ω, and ESPrpt 3 was used to generate the figure. The conserved residues are represented in red colour. The PDB ID 5DCM belongs to the C-terminal domain of the nisin resistance regulator NsrR from *Streptococcus agalactiae*; 4B09 belongs to the response regulator BaeR from *Escherichia coli* O6:H1; 4KNY belongs to the response regulator KdpE from *Escherichia coli* (strain K12); 2OQR: response regulator RegX3 from *Mycobacterium tuberculosis*; 5ED4 belongs to the response regulator PhoP from *Mycobacterium tuberculosis*; 1KGS belongs to the OmpR/PhoB homolog from *Thermotoga maritima*; and 4S04 belongs to the response regulator PmrA from *Klebsiella pneumonia* JM45.

showed that unphosphorylated GraR bound well to the promotor region of the *vraFG* operon (6).

4.2. Virtual screening

Drug-like compounds in the sdf format were retrieved from the ZINC database. Downloaded molecules were converted into pdbqt format using Open Babel. These molecules were used for virtual screening against GraR model utilizing AutoDock Vina in PyRx0.8. AutoDock Vina generated nine distinct poses along with the binding affinity of each ligand. Ligands that had high binding affinity were selected and inspected along with the corresponding interactions in PyMOL.

4.3. IC₅₀ and molecular properties calculations

The virtual molecules ZINC000049170029, ZINC000095509204, ZINC000067688459, ZINC000049169934, and ZINC000095352231 were predicted by pkCSM web-server (<http://biosig.unimelb.edu.au/pkcsml/>) to meet the Lipinski's rule of five criteria and ADMET properties. All the above compounds have a molecular weight of less than 500 Da, a LogP less than 5, and H-bond acceptors and donors of less than 10 and 5, respectively (Table 3). Further, the ADMET profile of these molecules was evaluated using pkCSM to predict the overall risks

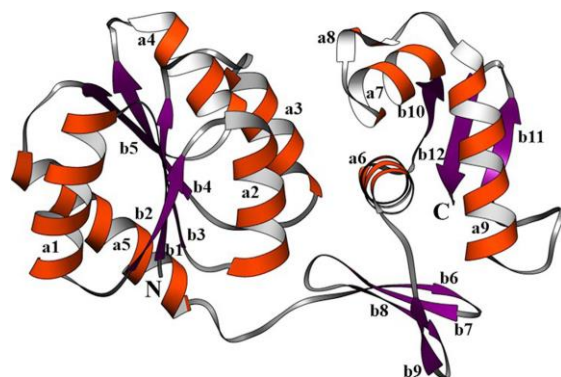


Figure 3. The computer-aided structure of GraR protein obtained from SWISS-MODEL and shown in ribbons using Chimera. The alpha-helices (a1-9), beta-sheets (b1-12), and loops are shown in orange, purple, and grey, respectively.

of absorption, distribution, metabolism, excretion, and toxicity as shown in Table 4. All of the five compounds showed good water solubility and fulfill the skin permeability criteria. Likewise, all the compounds showed significant Caco-2 permeability and also showed good human intestinal absorption of more than 90 percent. The steady-state volume of distribution (VD_{ss}) and unbound plasma fraction of all the compounds were below 1.8 and 0.6, respectively. None of the five compounds were found to be an inhibitor for the Cytochrome enzyme. The total clearance value of all the compounds was below 0.9. All the compounds showed a negative AMES, which indicates that they are non-mutagenic and non-carcinogenic. The XIAPin online server predicts that the above compounds have IC₅₀ values (the required amount of inhibitor to decline the enzymatic activity by 50 percent) in the range of 2.98 to 3.98 μ M as shown in Table 3. Further, binding of these molecules to GraR was cross-checked using another molecular docking program.

4.4. Molecular Docking

Molecular docking studies were employed to analyze the binding energy of the selected five compounds against GraR. All the compounds showed a binding affinity in the range of -6.38 to -10.24 kcal/mol, as shown in Table 5. All the docked compounds were predicted to bind

to the alpha4-beta5-alpha5 motif (Figure 6 and 7), which is shown to be involved in the phosphorylation-induced dimerization of OmpR/PhoB family of RRs (45). The GraR residues located in this motif: Arg67, Asn72, Pro73, Met90, Gly93, Ala94, Asp95, and Arg117 are conserved among the OmpR/PhoB proteins, as shown in Figure 2, and were predicted to interact with the screened compounds. The GraR-ligand complexes are stabilized by H-bonding and hydrophobic interactions (Figure 7 and 8): ZINC000095509204, ZINC000067688459, and ZINC000095352231 displayed H-bonding with Asp95 while ZINC000049170029 and ZINC000049169934 formed H-bond with Arg117, and Met90, respectively, (Figure 8). Except for ZINC000095509204, four out of the five compounds showed H-bonding with Arg67. HADDOCK docking results also show that 5 compounds (ZINC000049170029, ZINC0000-95509204, ZINC000067688459, ZINC00004-9169934, and ZINC000095352231) possess a good binding affinity for GraR protein as shown in Table 6. HADDOCK docking results are in accord with AutoDock results.

4.5. Molecular Dynamics simulation

Molecular dynamics (MD) simulation was performed to understand the variation at the atomistic level in GraR during the binding of each compound and determine stable and static interactions between the ligand and GraR. Molecular dynamics of GraR and GraR-ligand complexes were done in triplicates to explore the receptor-inhibitors interactions. In the current study, different parameters such as Root Mean Square Deviation (RMSD), Root Mean Square Fluctuation (RMSF), radius of gyration (Rg), Solvent Accessible Surface (SASA), and formation of hydrogen bond during the molecular simulation were characterized.

4.5.1. Root mean square deviation (RMSD)

The conformational changes and the dynamic stability of the C-alpha backbone atoms of GraR and GraR-ligand were studied by analyzing the RMSD during the simulation. RMSD

Table 2. The Ramachandran plot values of the GraR model obtained using PROCHECK

Ramachandran plot value	Percentage of residues
Most favoured regions	87.5
Additional allowed regions	12.0
Generously allowed regions	0.0
Disallowed regions	0.5

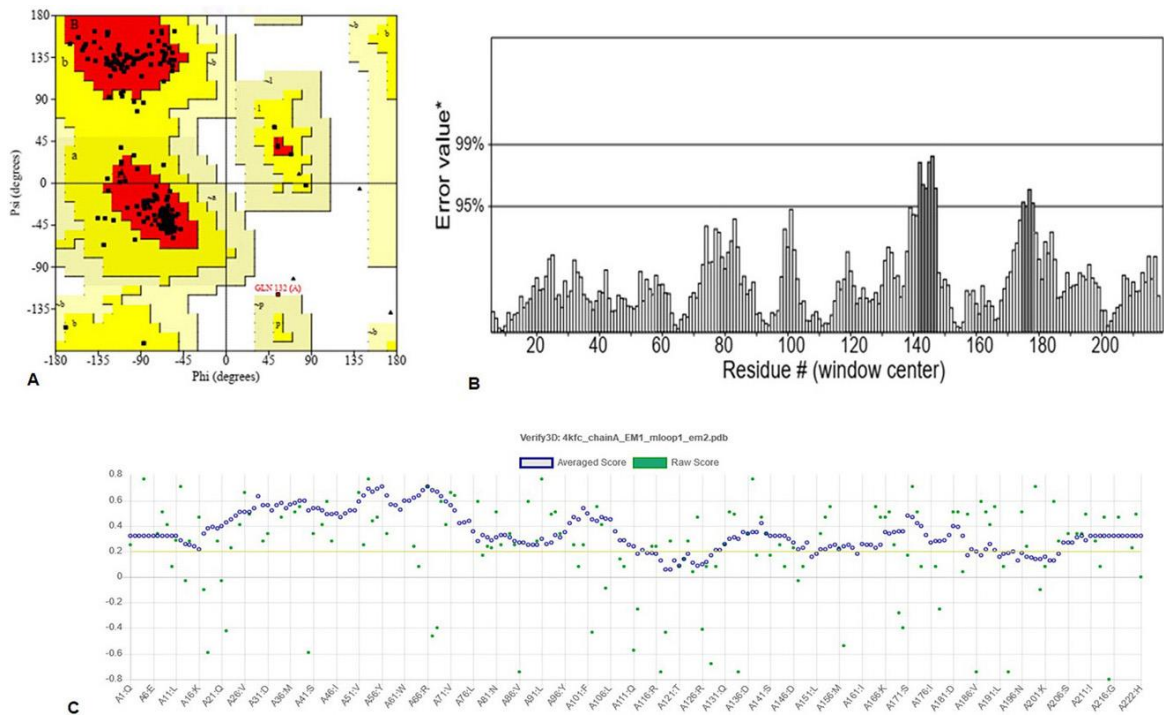


Figure 4. Assessment of the GraR model quality: (A) Ramachandran plot 3D model of GraR generated using PROCHECK. The most favoured region, allowed region, and disallowed region, is colored in red, yellow, and white, respectively. (B) ERRAT plot showing the quality of the GraR model. (C) The results obtained from the Verify-3D server, which calculated the compatibility of the 3D model with its 1D.

data shows that all the protein-ligand complexes attained equilibrium at 34 ns and systems were found to be stable for up to 100 ns as shown in Figure 9A. The average values of RMSD for GraR and GraR-ligand complexes are shown in Table 7. The RMSD values of GraR-ligand complexes are in the range of 0.41 nm to 0.44 nm, which is lesser than RMSD values obtained for GraR, as shown in Figure 9A. Ligand RMSD in GraR-ligand complexes are shown in Figure 9B. The average ligand RMSD is in the range of 0.05 to 0.1 nm, suggesting that binding of each compound to GraR is stable and static. Overall, the RMSD results show that the binding of each compound

to GraR is stable and does not affect the stability of the C-alpha backbone of the protein.

4.5.2. Root Mean Square Fluctuation (RMSF)

RMSF refers to the fluctuation in the C-alpha atoms from its average position throughout the molecular simulation. The secondary structure elements and loops indicate lower and higher RMSF, respectively. Here, we determined the residual mobility of the protein-ligand complex and plotted it against the amino acid number and fluctuation. The RMSF profile of the GraR-ligand complexes is almost comparable to GraR as

Table 3. Different physico-chemical properties (molecular weight, LogP, H-bond donor, H-bod acceptor) of the top scored binding affinity molecules fulfilling the Lipinski rule of five ($\log P \leq 5$, molecular weight ≤ 500 Da, number of hydrogen bond acceptors ≤ 10 , and number of hydrogen bond donors ≤ 5) with Inhibition Concentrations 50 (IC_{50})

S No:	ZINC ID	Molecular Weight (Da)	LogP	Rotatable Bonds	H-bond Acceptors	H-bond Donors	IC_{50} (μM)
1	ZINC000049170029	342.443	2.6287	4	6	0	3.93
2	ZINC000095509204	337.471	2.82552	2	5	1	2.98
3	ZINC000067688459	341.459	2.5761	5	6	2	3.56
4	ZINC000049169934	326.444	2.92852	3	5	0	3.98
5	ZINC000095352231	342.491	2.88042	4	6	0	3.62

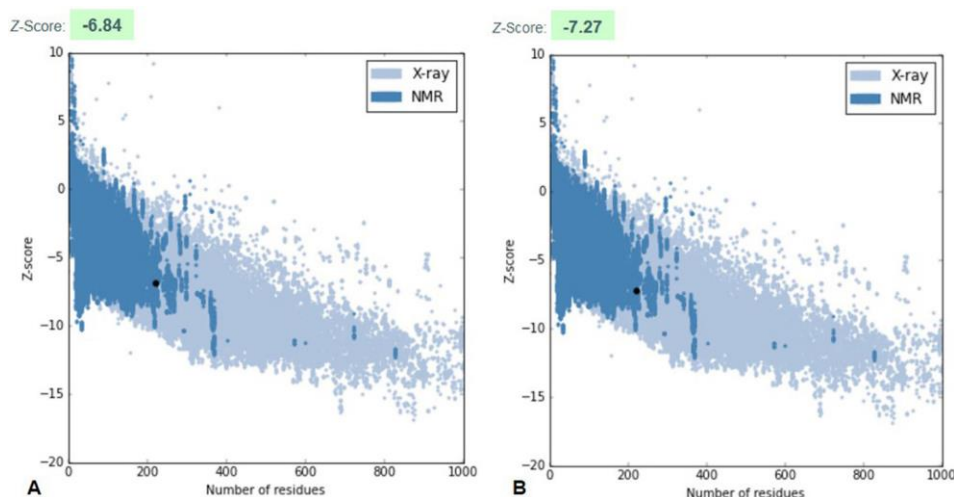


Figure 5. ProSA plot represents the overall quality of the model. (A) ProSA z-score of modeled GraR structure (B) ProSA z-score of the template, the response regulator KdpE structure from *Escherichia coli* (strain K12) (PDB ID: 4KFC).

shown in Figure 10. The average RMSF values of GraR-ligand complexes are in the range of 0.16 to 0.19 nm, which is smaller than GraR alone, as shown in Table 7. Therefore, the overall RMSF data indicate that each compound formed a stable complex with GraR and did not fluctuate in the binding site.

4.5.3. Radius of gyration (Rg)

Radius of gyration (Rg) indicates the overall compactness of the protein during the molecular dynamics. A smaller Rg value signifies a stably folded protein. The GraR-ligand complexes exhibit smaller Rg values as compared to the GraR protein, as shown in Figure

11. Protein-ligand complexes reveal an average Rg value in the range of 1.92 to 2.00 nm which is lesser than GraR, as shown in Table 7. These Rg results confirm that binding of each compound to GraR results in the formation of stable complexes.

4.5.4. Solvent Accessible Surface Area (SASA)

Polar and non-polar interactions of atoms contribute to the solvation free energy of a protein. SASA displays the probe of the center of the solvent molecule as it covers the surface of the receptor molecule. SASA of a protein decreases with increment in compactness of protein, so variation in

Table 4. The ADMET profile of the selected lead compounds

Provide title	Properties	ZINC0000 95352231	ZINC0000 49169934	ZINC0000 49170029	ZINC0000 95509204	ZINC0000 67688459
Absorption	Water solubility	-2.575	-2.785	-2.603	-2.852	-2.645
	Caco-2 permeability	0.895	1.292	1.163	0.982	0.998
	Intestinal absorption (human)	96.317	94.691	94.777	90.758	93.625
	Skin Permeability	-2.886	-3.01	-2.976	-2.907	-3.023
	P-glycoprotein substrate	Yes	Yes	Yes	Yes	Yes
	P-glycoprotein I inhibitor	No	No	Yes	No	No
	P-glycoprotein II inhibitor	No	No	No	No	No
Distribution	VDss (human)	0.059	1.793	1.522	1.012	1.039
	Fraction unbound (human)	0.524	0.345	0.317	0.549	0.597
	CNS permeability	-2.944	-2.149	-2.47	-2.027	-2.978
Metabolism	CYP2D6 substrate	No	No	No	No	No
	CYP1A2 inhibitor	Yes	Yes	Yes	No	Yes
	CYP2C19 inhibitor	No	No	No	No	No
	CYP2C9 inhibitor	No	No	No	No	No
	CYP3A4 inhibitor3	No	No	No	No	No
Excretion	Total Clearance	0.781	0.735	0.696	0.63	0.866
	Renal OCT2 substrate	No	Yes	Yes	No	No
Toxicity	AMES toxicity	No	No	No	No	No
	Max. tolerated dose (human)	0.112	-0.513	-0.498	-0.823	-0.513
	Oral Rat Acute Toxicity (LD50)	2.659	3.072	2.818	2.596	3.054
	Oral Rat Chronic Toxicity (LOAEL)	1.597	1.423	1.45	1.043	0.564
	Skin Sensitisation	No	No	No	No	No
	Minnow toxicity	1.735	1.777	1.193	1.263	1.354

SASA can predict the change in the structure of a protein. SASA plot shows that values of protein-ligand complexes are smaller compared to the native protein, as shown in Figure 12. The average SASA values of GraR-ligand complexes are in the range of 122.7 to 131.7 nm², which is smaller than GraR (133.1 nm²). SASA results suggest that the GraR-ligand complexes are more stable compared to GraR.

4.5.5. Hydrogen bond analysis

A hydrogen bond between an acceptor and a donor atom was generated within a distance and an angle range of 3.5 Å and 120°, respectively. The g_hbond tool of gromacs was utilized to predict the number of hydrogen bonds and distribution pattern in native protein and protein-inhibitor(s) complexes. Intra-protein

hydrogen bond graph was plotted to calculate the stability of GraR and GraR-ligand complexes as shown in Figure 13A. The GraR-ligand complexes exhibit more intra-protein hydrogen bonds compared to GraR, as shown in Figure 13B. In average, the number of the Intra-protein hydrogen bonds in GraR-ligand complexes is in the range of 174.2 to 181.1, while in GraR there are about 169.9 intra-protein hydrogen bonds, as shown in Table 7. Investigation of the inter-molecular hydrogen bond indicates that GraR-ligand complexes possess the minimum number of three hydrogen bonds during the molecular simulation, as shown in Figure 13C. The distribution of the hydrogen bond length depicts that GraR-ligand complexes form hydrogen bond from high to low affinity, which is related to GraR, as shown in Figure 13D. Overall, investigation of

Identification of potent inhibitors against GraR

Table 5. The binding affinities (kcal/mol) of the selected compounds with the interacting residues in GraR predicted from the molecular docking studies

S No:	ZINC ID	Binding affinity (kcal/mol)		Interacting residues	
		AutoDock Vina	AutoDock Tool	H-bond	Hydrophobic
1	ZINC000049170029	-7.4	-10.24	Arg67, Arg117	Met90, Ala94, Val72, Pro73, Ile74, Phe121, Val118, Ile114
2	ZINC000095509204	-6.9	-8.5	Asp95	Met90, Leu92, Ala94, Phe121, Ile74, Pro73, Val72, Val118
3	ZINC000067688459	-6.8	-8.08	Arg67, Asp95, Arg117	Pro73, Val72, Val118, Met90, Ala94, Phe121
4	ZINC000049169934	-6.9	-6.93	Arg67, Met90	Met90, Ala94, Val72, Pro73, Val118, Phe121
5	ZINC000095352231	-7.0	-6.38	Arg67, Asp95	Met90, Ala94, Asn71, Val72, Pro73, Ile74, Phe121, Val118

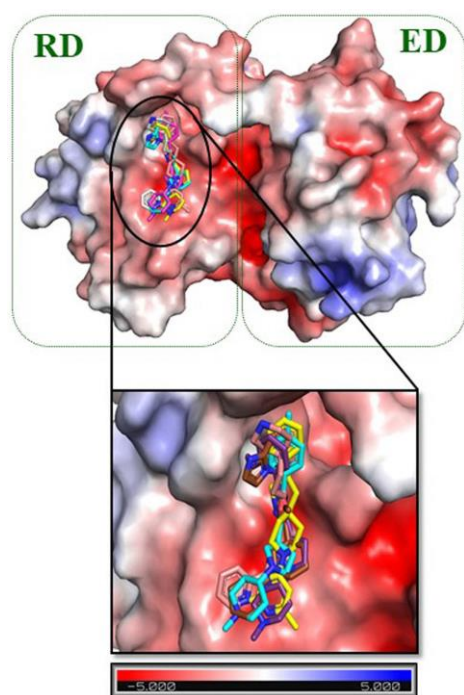


Figure 6. Electrostatic surface representation of GraR from *S. aureus*. The close-up view shows the binding pocket for ZINC000095509204, ZINC000067688459, ZINC000049169934, ZINC000095352231, and ZINC000049170029. These compounds are shown as carbon in gold, pink, cyan, brown, and purple respectively. Response regulator domain (RD) and effector domain (ED) are represented in the green dotted box. The electrostatic potential surface is color coded, red for negative and blue for positive electrostatic potential.

the hydrogen bonding shows that each compound tends to form stable GraR-ligand complex.

4.6. MMPBSA binding free energy calculation

The quantitative estimation of the binding free energy of ligand to a protein was calculated using the MMPBSA. The molecular dynamics trajectories of the last 20 ns were retrieved and used to generate the binding affinity of each complex. All the compounds show binding affinity in the range of -142.39 to -119.51 kJmol⁻¹, as shown in Table 8. The GraR-ZINC000049170029, GraR-ZINC000095509204, GraR-ZINC000067688459, GraR-ZINC000049169934, and GraR-ZINC000095352231 complexes exhibited a binding energy of -142.39 +/- 4.77, -133.41 +/- 23.32, -129.05 +/- 28.09, -130.44 +/- 6.56 and -119.51 +/- 4.78 kJmol⁻¹, respectively. The MMPBSA data confirmed that each compound can bind to GraR with a high binding affinity and result in the formation of a stable GraR-ligand complex.

5. DISCUSSION

A number of studies have shown that bacteria use signal-transduction pathways, such as those mediated by the two-component systems, in response to antibiotic-induced stress and as means to confer resistance to antibiotics (46-50). Here we focussed on the GraSR TCS, which responds to the action of CAMPs. (46-48, 51, 52). *S. aureus* infection causes the production of CAMPs by the host's immune system (53, 54). CAMPs have a net positive charge at the

Identification of potent inhibitors against GraR

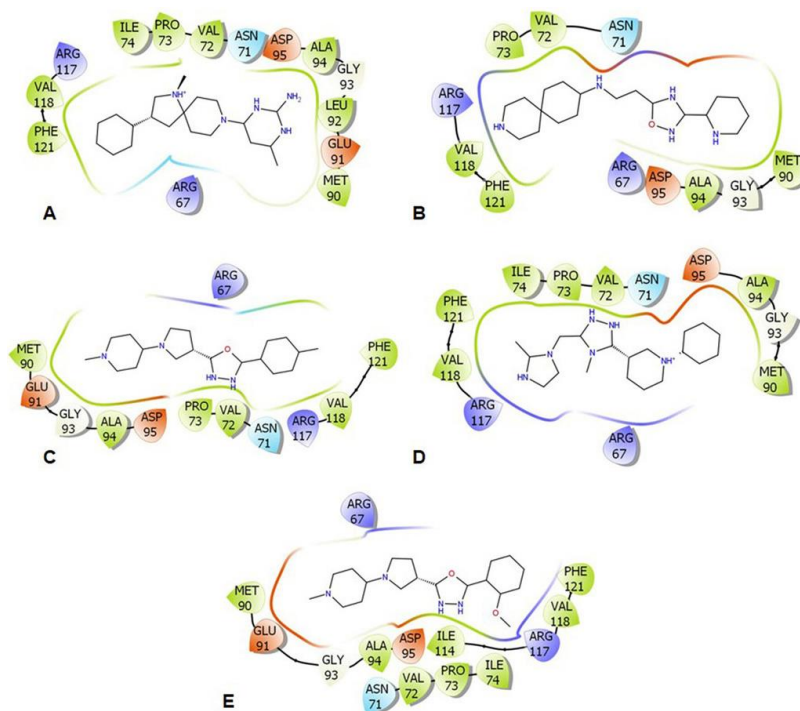


Figure 7. Illustrative representation of the protein-ligand interactions within 4 Å. (A) ZINC000095509204, (B) ZINC000067688459, (C) ZINC000049169934, (D) ZINC000095352231, and (E) ZINC000049170029. The color-coding features: green for hydrophobic, red for acidic, blue for basic, and cyan for polar residues.

physiological pH and may play a vital role in skin infections and life-threatening diseases such as pneumonia, endocarditis, meningitis, and toxic shock syndrome (1, 2). The response regulator protein GraR controls the expression of *mprF*, the *dltABCD*, and *vraFG* operons, the gene products of these operons are involved in resistance to several CAMPs.

In this study, the GraR structure was predicted and refined using SWISS model and SWISS PDB viewer. The refined model was assessed and validated using PROCHECK, VERIFY-3D, ERRAT, and ProSA. The domain analysis showed N- and C-terminal domains in the GraR in which C-terminal behaves as a DNA binding domain. Both domains are connected by a short loop of 7 residues (residues 122-128). The N-terminal domain (residues 1-121) is comprised of central parallel beta sheets (beta 1-5) surrounded by alpha1 and alpha5 helices on one face and alpha2-alpha4 helices on the other face

(Figure 3). This domain hosts the phosphorylation site, Asp51, the homodimerization site, and the highly conserved alpha4-beta5-alpha5 motif (6). The C-terminal domain (residues 129-224) hosts the DNA binding motif i.e. helix-turn-helix fold, which is conserved among the OmpR/PhoB family of proteins. The DNA-binding motif starts with four-stranded antiparallel beta-sheets and is followed by a helices bundled with two stranded anti-parallel beta-sheets. The GraR model shows two unique structural features: alpha4-beta5-alpha5 motif is fully exposed and not involved in the intra-domain interactions seen in other OmpR/PhoB proteins (43, 44), and the helix-turn-helix motif is also exposed. The latter feature is in agreement with previous *in vitro* studies of GraR DNA-binding activity (6).

The molecular docking and simulations studies were utilized to predict the efficiency of ligands binding to protein (55-58). Virtual screening is a powerful technique to identify

Identification of potent inhibitors against GraR

Table 6. Molecular docking analysis of GraR with ZINC000049170029, ZINC000095509204, ZINC000067688459, ZINC000049169934 and ZINC000095352231 by using HADDOCK

S No:	Compounds	HADDOCK Score	Van der wall Energy (kcal/mol)	Electrostatic Energy (kcal/mol)	Desolvation Energy (kcal/mol)
1.	ZINC000049170029	-86.0 +/- 4.9	-15.5 +/- 4.8	-406.5 +/- 37.0	-3.6 +/- 3.1
2.	ZINC000095509204	-72.0 +/- 2.4	-21.2 +/- 2.3	-169.8 +/- 7.5	-17.2 +/- 4.5
3.	ZINC000067688459	-70.8 +/- 1.6	-19.8 +/- 0.8	-157.8 +/- 5.8	-20.6 +/- 1.8
4.	ZINC000049169934	-59.8 +/- 2.8	-21.5 +/- 2.8	-111.8 +/- 11.6	-17.4 +/- 5.6
5.	ZINC000095352231	-53.6 +/- 3.1	-21.2 +/- 2.3	-78.7 +/- 10.9	-17.3 +/- 2.3

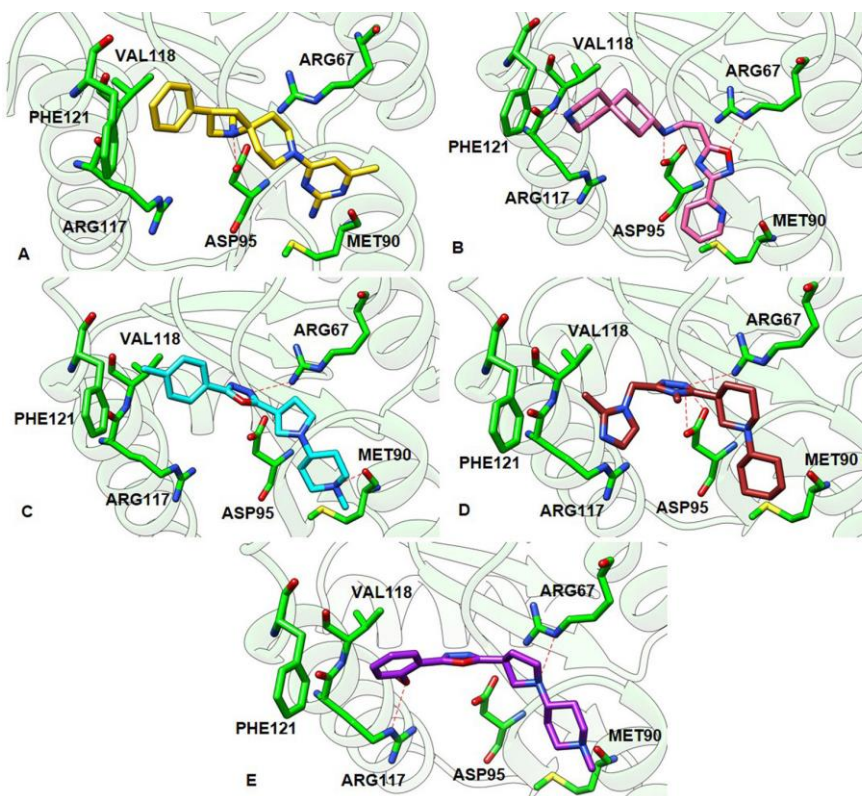


Figure 8. The best and the most stable binding conformation inferred from docking of the hit compounds against the constructed 3D model of GraR. (A) ZINC000095509204 (gold), (B) ZINC000067688459 (pink), (C) ZINC000049169934 (cyan), (D) ZINC000095352231 (brown), and (E) ZINC000049170029 (purple). The hydrogen bonds between the ligands and the receptor are shown as red dashed lines.

potential lead compounds in the field of drug discovery (59-61). Drug-like compounds of the ZINC database were screened against a validated model of GraR using AutoDock Vina in PyRx0.8. The binding conformation of the ligand and its interaction with the dimerization interface residues, along with the binding energy were

considered important factors for the selection of the best-docked conformation. A total of 5 compounds: ZINC000049170029, ZINC000095509204, ZINC000067688459, ZINC000049169934, and ZINC000095352231 were selected on the basis of the binding energy. Furthermore, visual inspection of the protein-

Identification of potent inhibitors against GraR

Table 7. The average values of root mean square deviation (RMSD), root mean square fluctuation (RMSF), radius of gyration, SASA and intra-H bond for GraR and GraR-ligand complexes for molecular simulation of 100 nano seconds (ns)

S No:	Compounds	Average Protein RMSD (nm)	Average ligand RMSD (nm)	Average RMSF (nm)	Average Radius of gyration (nm)	Average SASA (nm) ²	Intra-protein H-bonds
1.	GraR	0.46	-----	0.21	2.04	133.1	169.9
2.	ZINC000049170029	0.41	0.05	0.16	1.92	122.7	179.5
3.	ZINC000095509204	0.44	0.07	0.18	1.96	129.4	181.1
4.	ZINC000067688459	0.44	0.09	0.17	2.00	128.5	174.2
5.	ZINC000049169934	0.43	0.09	0.16	1.98	131.7	174.5
6.	ZINC000095352231	0.44	0.10	0.19	2.00	129.9	176.2

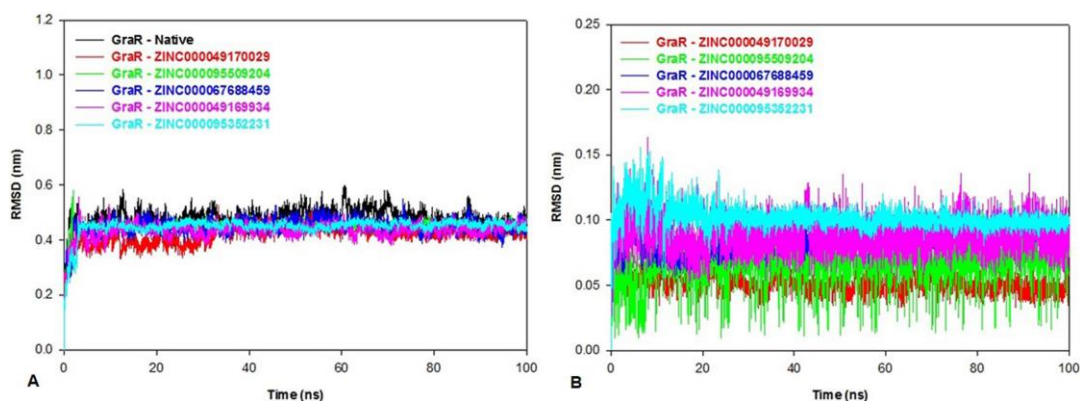


Figure 9. Root mean square deviation (RMSD) of the native protein, protein-ligand complexes and the ligand only. The RMSD plot of (A) GraR and GraR-ligand complexes, (B) Inhibitors/Ligands: ZINC000049170029 (red), ZINC000095509204 (green), ZINC000067688459 (blue), ZINC000049169934 (pink), and ZINC000095352231 (cyan) for 100 ns MD simulation.

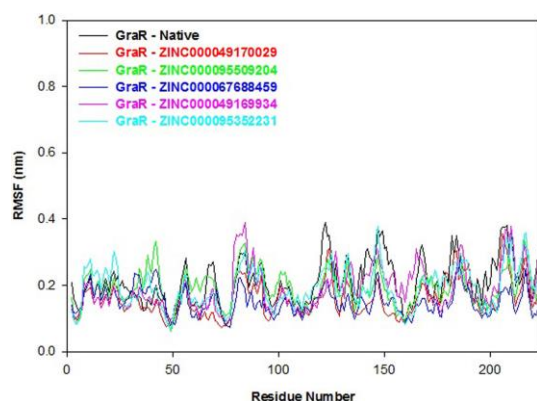


Figure 10. Root mean square fluctuation (RMSF) profiles of GraR (black), GraR-ZINC000049170029 (red), GraR-ZINC000095509204 (green), GraR-ZINC000067688459 (blue), GraR-ZINC000049169934 (pink), and GraR-ZINC000095352231 (cyan) during the molecular simulation of 100 ns.

compound complexes revealed that these compounds interact with Arg67, Asn72, Pro73, Met90, Gly93, Ala94, Asp95, and Arg117 residues of GraR, which are found in the alpha4-beta5-alpha5 motif, and are conserved among the OmpR/PhoB family of RRs.

The Lipinski rule of five was used to screen out the drug-like compound from the selected compounds. Drug-like properties such as molecular weight (less than 500 Da), H-bond donor (less than 5), H-bond acceptor (less than 10), and cLogP (less than 5) were analyzed for all the selected compounds. ADMET studies were performed to predict the pharmacokinetic properties and toxicity of drug-like compounds. The five selected compounds (ZINC000049170029, ZINC000095509204, ZINC000067688459, ZINC000049169934, and

Identification of potent inhibitors against GraR

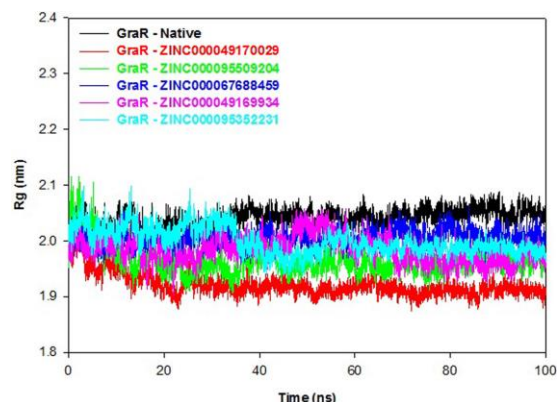


Figure 11. Radius of gyration graph of GraR and GraR-ligand complexes. The radius of gyration co-related with the compactness of the GraR protein during the molecular simulation time period of 100 ns.

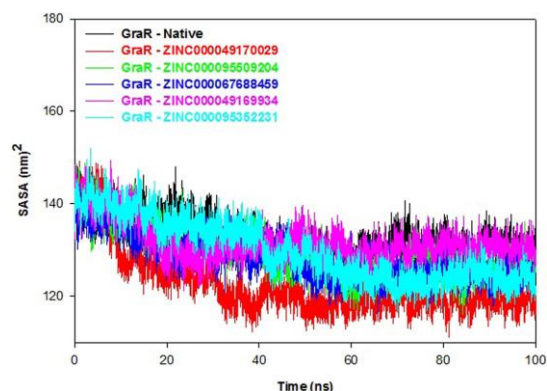


Figure 12. Solvent accessible surface area (SASA) profile of GraR and GraR-ligand complexes. SASA results of GraR, GraR-ZINC000049170029, GraR-ZINC000095509204, GraR-ZINC000067688459, GraR-ZINC000049169934, and GraR-ZINC000095352231 complexes at 300K for molecular simulation of 100 ns.

ZINC000095352231) fulfilled the Lipinski rule of five and ADMET criteria, and they showed low IC_{50} value. These studies suggested that the five selected compounds satisfied all the parameters for a potent inhibitor.

Further, the molecular docking studies were employed to study the interaction of the above compounds with GraR using AutoDock 4.2.6. and HADDOCK. The ZINC000049170029 compound showed the highest binding energy (-10.24 kcal/mol) and others showed slightly less binding energies, ranging from -8.5 kcal/mol to -

6.93 kcal/mol. Furthermore, the compounds ZINC000067688459, ZINC000095509204, and ZINC000095352231 were predicted to form intermolecular hydrogen bonds with Asp95 of GraR, while ZINC000049170029 and ZINC000049169934 were predicted to form intermolecular hydrogen bonds with Arg117 and Met90 of GraR, respectively, as shown in Figure 8. The docking study also predicted that all the five compounds are surrounded by hydrophobic residues in GraR (Val72, Pro73, Met90, Ala94, Val118, and Phe121) (Figure 7). From these results, it can be inferred that the hydrogen bonds and the hydrophobic interactions are likely to provide stability protein ligand complex. The best binding modes of all these compounds, generated by AutoDock, AutoDock Vina and HADDOCK, were almost identical. Hereafter, we speculate that these compounds may bind specifically to the GraR protein to inhibit its dimerization upon phosphorylation.

Molecular dynamics simulation was performed to understand the structural and conformational changes in the protein-ligand complex. RMSD of GraR-ligand complexes were smaller than GraR, suggesting that binding of each compound to GraR results in the formation of a stable complex. The overall values of RMSF indicate that the predicted inhibitor(s) was(were) well fitted into GraR without causing any structural fluctuations in the protein-ligand complex. The smaller Rg value of GraR-ligand complex in comparison to that of GraR suggests that the protein-ligand complexes are compactly packed and stable. SASA analysis also revealed that binding of these compounds to GraR tends to make the protein more compact as compared to GraR. The predicted inter-molecular hydrogen bonds in the protein-ligand complexes were shown to be stable throughout the molecular simulations and hence they are suggestive of stability of these complexes. MMPBSA data confirmed that all the compounds bound efficiently to GraR. The overall molecular dynamics simulations result conclude that all the screened compounds are potent molecules likely to prevent the homodimerization of GraR, which can then inhibit the GraSR response to CAMPs,

Identification of potent inhibitors against GraR

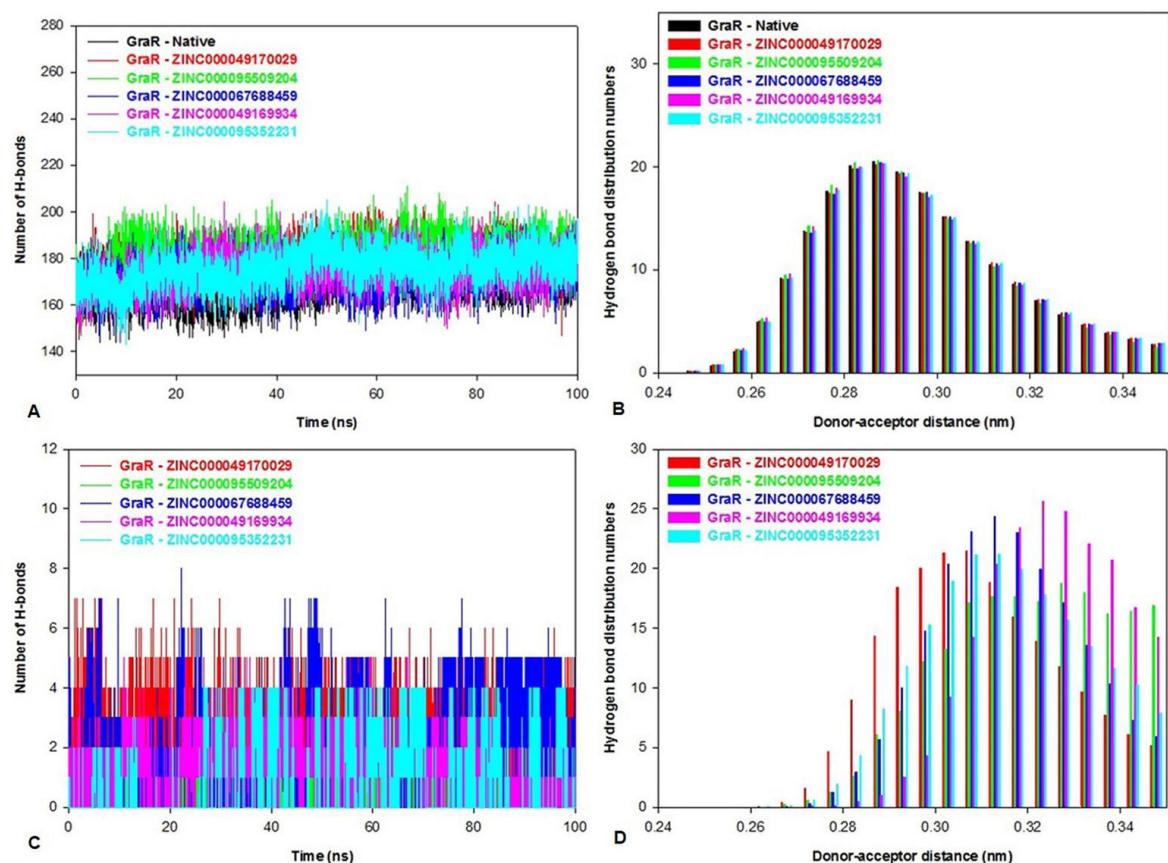


Figure 13. Bar representations of the hydrogen bond numbers and distribution in GraR, and GraR-ligand complexes. The hydrogen bond distribution is shown. (A) Intra-protein hydrogen bond numbers, (B) Intra-protein hydrogen bond distributions during the course of 100 ns simulation at 300 K, (C) Inter-molecular hydrogen bond numbers and (D) Inter-molecular hydrogen bond distributions during the course of 100 ns simulation at 300 K.

and lead to the re-sensitization of *S. aureus* to CAMPs.

6. CONCLUSION

S. aureus is a major human pathogen that has developed resistance against various antibiotics. TCSs respond to a specific environmental signal such as pH, nutrient levels, osmotic pressure, redox state, quorum-sensing proteins and antibiotics. GraR of *S. aureus* is an attractive target for drug development as its inhibition could reduce *in vivo* survival. A 3D model of GraR was predicted and further validated using several tools of SAVES server. To identify potent GraR-binding molecules, a structure-based virtual screening of GraR against

the ZINC database molecules was performed. The selected molecules were screened by assessing the pharmacophore properties such as Lipinski rule of five and ADMET, and IC₅₀. The molecular docking was used to analyze the interactions between the identified compounds and GraR. The molecular docking results showed that five compounds: ZINC000049170029, ZINC000095509204, ZINC000067688459, ZINC000049169934, and ZINC000095352231 interact at the dimerization interface residues of GraR through hydrogen bonding, hydrophobic and polar interactions as they have the aromatic ring with a charged group. The molecular dynamics study confirmed that the selected compounds bind to GraR efficiently and form stable GraR-ligand complexes. These lead

Table 8. The binding free energy calculations for the GraR-ligand complexes by molecular mechanic/Poisson-Boltzmann surface area (MMPBSA)

S No:	Compound	Van der Waals energy (kJ/mol)	Electrostatic energy (kJ/mol)	Polar solvation energy (kJ/mol)	SASA energy (kJ/mol)	Binding energy (kJ/mol)
1	ZINC000049170029	-107.39 +/- 1.46	-205.39 +/- 5.81	17.14 +/- 4.89	-15.74 +/- 0.14	-142.39 +/- 4.77
2	ZINC000095509204	-50.44 +/- 9.32	-205.85 +/- 32.66	129.77 +/- 20.29	-6.81 +/- 1.13	-133.41 +/- 23.32
3	ZINC000067688459	-68.59 +/- 6.12	-205.53 +/- 71.43	155.48 +/- 51.85	-10.41 +/- 0.82	-129.05 +/- 28.09
4	ZINC000049169934	-61.26 +/- 1.46	-186.74 +/- 8.77	127.52 +/- 12.61	-13.85 +/- 0.13	-130.44 +/- 6.56
5	ZINC000095352231	-94.77 +/- 2.62	-175.24 +/- 11.97	164.56 +/- 10.07	-13.96 +/- 0.29	-119.51 +/- 4.78

compounds can be further validated *in vitro* studies and subsequently can be utilized for the development of antimicrobial compounds against *S. aureus*.

7. ACKNOWLEDGMENTS

I am the corresponding author of this manuscript and I declare no conflict of interest. PD and VD contributed equally to this paper. PD thanks Ministry of Human Resource Development and VD thanks Department of Biotechnology (DBT/2015/IIT-R/349) for financial support.

8. REFERENCES

1. M. Falord, U. Mäder, A. Hiron, M. Debarbouille and T. Msadek: Investigation of the Staphylococcus aureus GraSR regulon reveals novel links to virulence, stress response and cell wall signal transduction pathways. PloS One, 6(7), e21323 (2011). DOI: 10.1371/journal.pone.0021323 PMID:21765893 PMCID:PMC3128592
2. Q. Liu, W. S. Yeo and T. Bae: The SaeRS two-component system of Staphylococcus aureus. Genes, 7(10), 81 (2016) DOI: 10.3390/genes7100081 PMID:27706107 PMCID:PMC5083920
3. R. Rashid, M. Veleba and K. A. Kline: Focal targeting of the bacterial envelope by antimicrobial peptides. Front Cell Dev Biol, 4, 55 (2016) DOI: 10.3389/fcell.2016.00055 PMID:27376064 PMCID:PMC4894902
4. K. Nawrocki, E. Crispell and S. McBride: Antimicrobial peptide resistance mechanisms of gram-positive bacteria. Antibiotics-Basel, 3(4), 461-492 (2014) DOI: 10.3390/antibiotics3040461 PMID:25419466 PMCID:PMC4239024
5. A. Narayanan, S. Kumar, A. N. Evrard, L. N. Paul and D. A. Yernool: An asymmetric heterodomain interface stabilizes a response regulator-DNA complex. Nat Commun, 5, 3282 (2014) DOI: 10.1038/ncomms4282 PMID:24526190 PMCID:PMC4399498
6. U. Muzamal, D. Gomez, F. Kapadia and D. Golemi-Kotra: Diversity of two-component systems: insights into the signal transduction mechanism by the Staphylococcus aureus two-component system GraSR. F1000Research, 3 (2014)

- DOI: 10.12688/f1000research.5512.2
PMid:25685323 PMCID:PMC4314665
7. Y.-C. Lou, T.-H. Weng, Y.-C. Li, Y.-F. Kao, W.-F. Lin, H.-L. Peng, S.-H. Chou, C.-D. Hsiao and C. Chen: Structure and dynamics of polymyxin-resistance-associated response regulator PmrA in complex with promoter DNA. *Nat Commun*, 6, 8838 (2015)
DOI: 10.1038/ncomms9838
PMid:26564787 PMCID:PMC4660055
8. S. Menon and S. Wang: Structure of the response regulator PhoP from *Mycobacterium tuberculosis* reveals a dimer through the receiver domain. *Biochemistry*, 50(26), 5948-5957 (2011)
DOI: 10.1021/bi2005575
PMid:21634789 PMCID:PMC3133661
9. B. F. Volkman, D. Lipson, D. E. Wemmer and D. Kern: Two-state allosteric behavior in a single-domain signaling protein. *Science*, 291(5512), 2429-2433 (2001)
DOI: 10.1126/science.291.5512.2429
PMid:11264542
10. M. Fridman, G. D. Williams, U. Muzamal, H. Hunter, K. M. Siu and D. Golemi-Kotra: Two unique phosphorylation-driven signaling pathways crosstalk in *Staphylococcus aureus* to modulate the cell-wall charge: Stk1/Stp1 meets GraSR. *Biochemistry*, 52(45), 7975-7986 (2013)
DOI: 10.1021/bi401177n
PMid:24102310
11. Y. T. Tang, R. Gao, J. J. Havranek, E. A. Groisman, A. M. Stock and G. R. Marshall: Inhibition of Bacterial Virulence: Drug-Like Molecules Targeting the *Salmonella enterica* PhoP Response Regulator. *Chem Biol Drug Des*, 79(6), 1007-1017 (2012)
DOI: 10.1111/j.1747-0285.2012.01362.x
PMid:22339993 PMCID:PMC3445336
12. F. Trajtenberg, D. Albanesi, N. Ruétalo, H. Botti, A. E. Mechaly, M. Nieves, P. S. Aguilar, L. Cybulski, N. Larrieux and D. de Mendoza: Allosteric activation of bacterial response regulators: the role of the cognate histidine kinase beyond phosphorylation. *MBio*, 5(6), e02105-14 (2014)
DOI: 10.1128/mBio.02105-14
PMid:25406381 PMCID:PMC4251995
13. S. F. Altschul, W. Gish, W. Miller, E. W. Myers and D. J. Lipman: Basic local alignment search tool. *J Mol Biol*, 215(3), 403-410 (1990)
DOI: 10.1016/S0022-2836(05)80360-2
14. U. Consortium: UniProt: a worldwide hub of protein knowledge. *Nucleic Acids Res*, 47(D1), D506-D515 (2018)
DOI: 10.1093/nar/gky1049
PMid:30395287 PMCID:PMC6323992
15. P. Gouet, E. Courcelle, D. I. Stuart and F. M. J. Drenth: ESPript: analysis of multiple sequence alignments in PostScript. *Bioinformatics (Oxford, England)*, 15(4), 305-308 (1999)
DOI: 10.1093/bioinformatics/15.4.305
PMid:10320398
16. F. Sievers, A. Wilm, D. Dineen, T. J. Gibson, K. Karplus, W. Li, R. Lopez, H. McWilliam, M. Remmert and J. Söding: Fast, scalable generation of high-quality protein multiple sequence alignments using Clustal Omega. *Mol Syst Biol*, 7(1), 539 (2011)
DOI: 10.1038/msb.2011.75
PMid:21988835 PMCID:PMC3261699
17. A. L. Mitchell, T. K. Attwood, P. C.

- Babbitt, M. Blum, P. Bork, A. Bridge, S. D. Brown, H.-Y. Chang, S. El-Gebali and M. I. Fraser: InterPro in 2019: improving coverage, classification and access to protein sequence annotations. *Nucleic Acids Res*, 47(D1), D351-D360 (2018)
DOI: 10.1093/nar/gky1100
PMid:30398656 PMCID:PMC6323941
18. C. J. Sigrist, E. De Castro, L. Cerutti, B. A. CuChe, N. Hulo, A. Bridge, L. Bougueleret and I. Xenarios: New and continuing developments at PROSITE. *Nucleic Acids Res*, 41(D1), D344-D347 (2012)
DOI: 10.1093/nar/gks1067
PMid:23161676 PMCID:PMC3531220
19. A. Marchler-Bauer, M. K. Derbyshire, N. R. Gonzales, S. Lu, F. Chitsaz, L. Y. Geer, R. C. Geer, J. He, M. Gwadz and D. I. Hurwitz: CDD: NCBI's conserved domain database. *Nucleic Acids Res*, 43(D1), D222-D226 (2014)
DOI: 10.1093/nar/gku1221
PMid:25414356 PMCID:PMC4383992
20. T. Schwede, J. Kopp, N. Guex and M. C. Peitsch: SWISS-MODEL: an automated protein homology-modeling server. *Nucleic Acids Res*, 31(13), 3381-3385 (2003)
DOI: 10.1093/nar/gkg520
PMid:12824332 PMCID:PMC168927
21. A. Fiser and R. K. G. Do: Modeling of loops in protein structures. *Protein Sci*, 9(9), 1753-1773 (2000)
DOI: 10.1110/ps.9.9.1753
PMid:11045621 PMCID:PMC2144714
22. N. Guex and M. C. Peitsch: SWISS-MODEL and the Swiss-Pdb Viewer: an environment for comparative protein modeling. *electrophoresis*, 18(15), 2714-2723 (1997)
DOI: 10.1002/elps.1150181505
PMid:9504803
23. C. Colovos and T. O. Yeates: Verification of protein structures: patterns of nonbonded atomic interactions. *Protein Sci*, 2(9), 1511-1519 (1993)
DOI: 10.1002/pro.5560020916
PMid:8401235 PMCID:PMC2142462
24. D. Eisenberg, R. Lüthy and J. U. Bowie: (20) VERIFY3D: assessment of protein models with three-dimensional profiles. In: *Method Enzymol*. Elsevier, (1997)
DOI: 10.1016/S0076-6879(97)77022-8
25. R. A. Laskowski, M. W. MacArthur, D. S. Moss and J. M. Thornton: PROCHECK: a program to check the stereochemical quality of protein structures. *J Appl Crystallogr*, 26(2), 283-291 (1993)
DOI: 10.1107/S0021889892009944
26. M. Wiederstein and M. J. Sippl: ProSA-web: interactive web service for the recognition of errors in three-dimensional structures of proteins. *Nucleic Acids Res*, 35(suppl_2), W407-W410 (2007)
DOI: 10.1093/nar/gkm290
PMid:17517781 PMCID:PMC1933241
27. W. L. DeLano: Pymol: An open-source molecular graphics tool. *CCP4 Newsletter On Protein Crystallography*, 40(1), 82-92 (2002)
28. E. F. Pettersen, T. D. Goddard, C. C. Huang, G. S. Couch, D. M. Greenblatt, E. C. Meng and T. E. Ferrin: UCSF Chimera-a visualization system for exploratory research and analysis. *J Comput Chem*, 25(13), 1605-1612 (2004)

- DOI: 10.1002/jcc.20084
PMid:15264254
29. D. Van Der Spoel, E. Lindahl, B. Hess, G. Groenhof, A. E. Mark and H. J. Berendsen: GROMACS: fast, flexible, and free. *J Comput Chem*, 26(16), 1701-1718 (2005)
DOI: 10.1002/jcc.20291
PMid:16211538
30. W. F. van Gunsteren, S. Billeter, A. Eising, P. H. Hünenberger, P. Krüger, A. E. Mark, W. Scott and I. G. Tironi: Biomolecular simulation: the {GROMOS96} manual and user guide (1996)
31. T. Sterling and J. J. Irwin: ZINC 15-ligand discovery for everyone. *J Chem Inf Model*, 55(11), 2324-2337 (2015)
DOI: 10.1021/acs.jcim.5b00559
PMid:26479676 PMCID:PMC4658288
32. S. Dallakyan and A. J. Olson: Small-molecule library screening by docking with PyRx. In: *Chemical Biology*. Springer, 243-250 (2015)
DOI: 10.1007/978-1-4939-2269-7_19
PMid:25618350
33. N. M. O'Boyle, M. Banck, C. A. James, C. Morley, T. Vandermeersch and G. R. Hutchison: Open Babel: An open chemical toolbox. *J Cheminformatics*, 3(1), 33 (2011)
DOI: 10.1186/1758-2946-3-33
PMid:21982300 PMCID:PMC3198950
34. O. Trott and A. J. Olson: AutoDock Vina: improving the speed and accuracy of docking with a new scoring function, efficient optimization, and multithreading. *J Comput Chem*, 31(2), 455-461 (2010)
DOI: 10.1002/jcc.21334
PMid:19499576 PMCID:PMC3041641
35. D. E. Pires, T. L. Blundell and D. B. Ascher: pkCSM: predicting small-molecule pharmacokinetic and toxicity properties using graph-based signatures. *J Comput Chem*, 58(9), 4066-4072 (2015)
DOI: 10.1021/acs.jmedchem.5b00104
PMid:25860834 PMCID:PMC4434528
36. G. M. Morris, R. Huey, W. Lindstrom, M. F. Sanner, R. K. Belew, D. S. Goodsell and A. J. Olson: AutoDock4 and AutoDockTools4: Automated docking with selective receptor flexibility. *J Comput Chem*, 30(16), 2785-2791 (2009)
DOI: 10.1002/jcc.21256
PMid:19399780 PMCID:PMC2760638
37. S. J. De Vries, M. Van Dijk and A. M. Bonvin: The HADDOCK web server for data-driven biomolecular docking. *Nat Protoc*, 5(5), 883 (2010)
DOI: 10.1038/nprot.2010.32
PMid:20431534
38. Z. Kurkcuoglu, P. I. Koukos, N. Citro, M. E. Trellet, J. Rodrigues, I. S. Moreira, J. Roel-Touris, A. S. Melquiond, C. Geng and J. Schaarschmidt: Performance of HADDOCK and a simple contact-based protein-ligand binding affinity predictor in the D3R Grand Challenge 2. *J Comput Aid Mol Des*, 32(1), 175-185 (2018)
DOI: 10.1007/s10822-017-0049-y
PMid:28831657 PMCID:PMC5767195
39. W. F. van Gunsteren, S. R. Billeter, A. A. Eising, P. H. Hünenberger, P. Krüger, A. E. Mark, W. R. Scott and I. G. Tironi: Biomolecular simulation: the {GROMOS96} manual and user guide (1996)
40. A. W. Schüttelkopf and D. M. Van Aalten: PRODRG: a tool for high-throughput

- crystallography of protein-ligand complexes. *Acta Crystallographica Section D: Acta Crystallogr D*, 60(8), 1355-1363 (2004)
DOI: 10.1107/S0907444904011679
PMid:15272157
41. M. J. Abraham and J. E. Gready: Optimization of parameters for molecular dynamics simulation using smooth particle-mesh Ewald in GROMACS 4.5. *J Comput Chem*, 32(9), 2031-2040 (2011)
DOI: 10.1002/jcc.21773
PMid:21469158
42. R. Kumari, R. Kumar, O. S. D. D. Consortium and A. Lynn: g_mmpbsa A GROMACS tool for high-throughput MM-PBSA calculations. *J Chem Inf Model*, 54(7), 1951-1962 (2014)
DOI: 10.1021/ci500020m
PMid:24850022
43. D. R. Buckler, Y. Zhou and A. M. Stock: Evidence of intradomain and interdomain flexibility in an OmpR/PhoB homolog from *Thermotoga maritima*. *Structure*, 10(2), 153-164 (2002)
DOI: 10.1016/S0969-2126(01)00706-7
44. E. Nowak, S. Panjikar, P. Konarev, D. I. Svergun and P. A. Tucker: The structural basis of signal transduction for the response regulator PrrA from *Mycobacterium tuberculosis*. *J Biol Chem*, 281(14), 9659-9666 (2006)
DOI: 10.1074/jbc.M512004200
PMid:16434396
45. R. Gao and A. M. Stock: Biological insights from structures of two-component proteins. *Annu Rev Microbiol*, 63, 133-154 (2009)
DOI: 10.1146/annurev.micro.-091208.073214
PMid:19575571 PMCID:PMC3645274
46. K. S. Choudhary, N. Mih, J. Monk, E. Kavvas, J. T. Yurkovich, G. Sakoulas and B. O. Palsson: The *Staphylococcus aureus* two-component system AgrAC displays four distinct genomic arrangements that delineate genomic virulence factor signatures. *Front Microbiol*, 9 (2018)
DOI: 10.3389/fmicb.2018.01082
PMid:29887846 PMCID:PMC5981134
47. H. Guo, J. W. Hall, J. Yang and Y. Ji: The SaeRS two-component system controls survival of *Staphylococcus aureus* in human blood through regulation of coagulase. *Front Cell Infect Microbiol*, 7, 204 (2017)
DOI: 10.3389/fcimb.2017.00204
PMid:28611950 PMCID:PMC5447086
48. J. N. Radin, J. L. Kelliher, P. K. P. Solorzano and T. E. Kehl-Fie: The two-component system ArlRS and alterations in metabolism enable *Staphylococcus aureus* to resist calprotectin-induced manganese starvation. *Plos Pathog*, 12(11), e1006040 (2016)
DOI: 10.1371/journal.ppat.1006040
PMid:27902777 PMCID:PMC5130280
49. A. Belcheva and D. Golemi-Kotra: A close-up view of the VraSR two-component system a mediator of *Staphylococcus aureus* response to cell wall damage. *J Biol Chem*, 283(18), 12354-12364 (2008)
DOI: 10.1074/jbc.M710010200
PMid:18326495
50. S. L. Kellogg, J. L. Little, J. S. Hoff and C. J. Kristich: Requirement of the CroRS two-component system for resistance to cell wall-targeting antimicrobials in *Enterococcus faecium*. *Antimicrob Agents Ch*, 61(5), e02461-16 (2017)
DOI: 10.1128/AAC.02461-16

- PMid:28223383 PMCID:PMC5404561
51. J. W. Hall, J. Yang, H. Guo and Y. Ji: The *Staphylococcus aureus* AirSR two-component system mediates reactive oxygen species resistance via transcriptional regulation of staphyloxanthin production. *Infect Immun*, 85(2), e00838-16 (2017)
DOI: 10.1128/IAI.00838-16
PMid:27872240 PMCID:PMC5278164
 52. T. Xue, Y. You, D. Hong, H. Sun and B. Sun: The *Staphylococcus aureus* KdpDE two-component system couples extracellular K⁺ sensing and Agr signaling to infection programming. *Infect Immun*, 79(6), 2154-2167 (2011)
DOI: 10.1128/IAI.01180-10
PMid:21422185 PMCID:PMC3125826
 53. H.-S. Joo and M. Otto: Mechanisms of resistance to antimicrobial peptides in staphylococci. *Bba-Biomembranes*, 1848(11), 3055-3061 (2015)
DOI: 10.1016/j.bbamem.2015.02.009
PMid:25701233 PMCID:PMC4539291
 54. S. Ryu, P. Song, C. Seo, H. Cheong and Y. Park: Colonization and infection of the skin by *S. aureus*: immune system evasion and the response to cationic antimicrobial peptides. *Int J Mol Sci*, 15(5), 8753-8772 (2014)
DOI: 10.3390/ijms15058753
PMid:24840573 PMCID:PMC4057757
 55. V. Dalal, P. Kumar, G. Rakhaminov, A. Qamar, X. Fan, H. Hunter, S. Tomar, D. Golemi-Kotra and P. Kumar: Repurposing an ancient protein core structure: structural studies on FmtA, a novel esterase of *staphylococcus aureus*. *J Mol Biol*, 431(17), 3107-3123 (2019)
DOI: 10.1016/j.jmb.2019.06.019
PMid:31260692
 56. N. Singh, V. Dalal and P. Kumar: Structure based mimicking of Phthalic acid esters (PAEs) and inhibition of hACMSD, an important enzyme of the tryptophan kynurenine metabolism pathway. *Int J Biol Macromol*, 108, 214-224 (2018)
DOI: 10.1016/j.ijbiomac.2017.12.005
PMid:29217180
 57. N. Singh, V. Dalal and P. Kumar: Molecular docking and simulation analysis for elucidation of toxic effects of dicyclohexyl phthalate (DCHP) in glucocorticoid receptor-mediated adipogenesis. *Mol Simulat*, 1-13 (2019)
DOI: 10.1080/08927022.2019.1662002
 58. N. Singh, V. Dalal, J. K. Mahto and P. Kumar: Biodegradation of phthalic acid esters (PAEs) and in silico structural characterization of mono-2-ethylhexyl phthalate (MEHP) hydrolase on the basis of close structural homolog. *J Hazard Mater*, 338, 11-22 (2017)
DOI: 10.1016/j.jhazmat.2017.04.055
PMid:28531656
 59. A. Malik, V. Dalal, S. Ankri and S. Tomar: Structural insights into *Entamoeba histolytica* arginase and structure-based identification of novel non-amino acid based inhibitors as potential antiamebic molecules. *Febs J*, 286, 4135-4155 (2019)
DOI: 10.1111/febs.14960
PMid:31199070
 60. G. Saini, V. Dalal, B. K. Savita, N. Sharma, P. Kumar and A. K. Sharma: Molecular docking and dynamic approach to virtual screen inhibitors against Esbp of *Candidatus Liberibacter asiaticus*. *J Mol Graph Model*, 92, 329-340 (2019)
DOI: 10.1016/j.jmgm.2019.08.012
PMid:31446203

61. H. Tarazi, E. Saleh and R. El-Awady: In-silico screening for DNA-dependent protein kinase (DNA-PK) inhibitors: Combined homology modeling, docking, molecular dynamic study followed by biological investigation. Biomed Pharmacother, 83, 693-703 (2016)
DOI: 10.1016/j.biopha.2016.07.044
PMid:27470570

Abbreviations: TCS: Two-component systems; CAMPs: cationic antimicrobial peptides; HK: histidine kinase; RR: response regulator; RD: receiver domain; ED: effector domain; WTA: wall teichoic acid; MD: molecular dynamics; MMPBSA: molecular mechanic/Poisson-Boltzmann surface area; UFF: Universal Force Field; VD: volume of distribution; RMSD: Root Mean Square Deviation; RMSF: Root Mean Square Fluctuation; SASA: Solvent Accessible Surface Area; ns: nano second.

Key Words: *Staphylococcus aureus*; Two-component system; Histidine kinase; Response regulator; GraR, CAMP, Molecular Dynamics Simulation

Send correspondence to: Pravindra Kumar, Ph. Department of Biotechnology, Indian Institute of Technology Roorkee, India – 247667, Telephone: 91-1332-286286, Fax: 91-1332-273560, E-mail: pravshai@gmail.com